Redesigning Experimental Equipment for Determining Peak Pressure in a Simulated Tank Car Transfer Line

by

Richard A. Diaz

SUBMITTED TO THE DEPARTMENT OF MECHANICAL ENGINEERING IN PARTIAL FULFILLMENT OF THE REQUIREMENTS FOR THE DEGREE OF

BACHELOR OF SCIENCE
AT THE
MASSACHUSETTS INSTITUTE OF TECHNOLOGY

JUNE 2007

Author: ______________________________
Department of Mechanical Engineering
May 14, 2007

Certified by: ______________________________
Professor Doug Hart
Professor of Mechanical Engineering
Thesis Supervisor

Accepted by: ______________________________
John H. Lienhard V
Professor of Mechanical Engineering
Chairman, Undergraduate Thesis Committee

Redesigning Experimental Equipment for Determining Peak Pressure in a Simulated Tank Car Transfer Line
by
Richard Diaz

Submitted to the Department of Mechanical Engineering on May 11, 2007 in partial fulfillment of the requirements for the Degree of Bachelor of Science in Mechanical Engineering

Abstract

When liquids are transported from storage tanks to tank cars, improper order of valve openings can cause pressure surges in the transfer line. To model this phenomenon and predict the peak pressures in such a transfer line, a laboratory setup consisting of a pressurized water storage tank connected to different segments of pipe by ball valves was constructed. By varying parameters including water height within the tank, transfer line length, and applied driving pressure, the most critical variable was determined to be driving pressure. The hydrostatic pressure from the difference in water height was negligible and this fact was evident without the need for experimental verification. This setup therefore allowed for even fewer parameters to be tested. Due to the poor condition of the experiment because of age and corrosion along with the few insights the setup provided, the experiment needed to be updated. The newer version is designed to allow students to have more choice in what parameters they wish to test, with pipe segments of different length as well as different diameter with various impedances. To address spatial and practical considerations, the new design was assembled in PVC piping. This mockup proved useful in discovering inadequacies in the design that had not been considered.

While the mockup proved that the design was safe to use at the operating pressures within the 2.672 laboratory for which the experiment is intended, it also proved that there were important factors influencing the aesthetics of the experiment that had been considered secondary to the safety. To add complexity to the problem, the design included clear segments of pipe near the ends in which the water hammer would oscillate so that digital imaging analysis could later be implemented. However, the increase in pipe length to hide the pressure tank below the table also caused the air pressure required to drive the oscillations in the clear section of pipe to be much higher than operating pressure. As this build was considered as a mockup, these problems have been noted so future designs for the final experiment to be used in the 2.672 classroom can address these problems.

Professor Douglas Hart
Professor of Mechanical Engineering
Thesis Supervisor

Introduction

Highly corrosive or volatile liquids are often kept in high pressure tanks at storage facilities before being loaded into tank cars for distribution. The high pressure of the tank is used to drive the liquid from the tank into the car. When transferring the liquid between the tank and the car, it is favorable to open the valve at the car first so that the liquid forces the air out of the line between the valves at the tank and the car (Valves A and B, respectively in Figure 1). If valve A is opened first, the sudden surge of liquid into the closed section of pipe compresses the air against the second valve and causes pressure surges within this section of pipe.

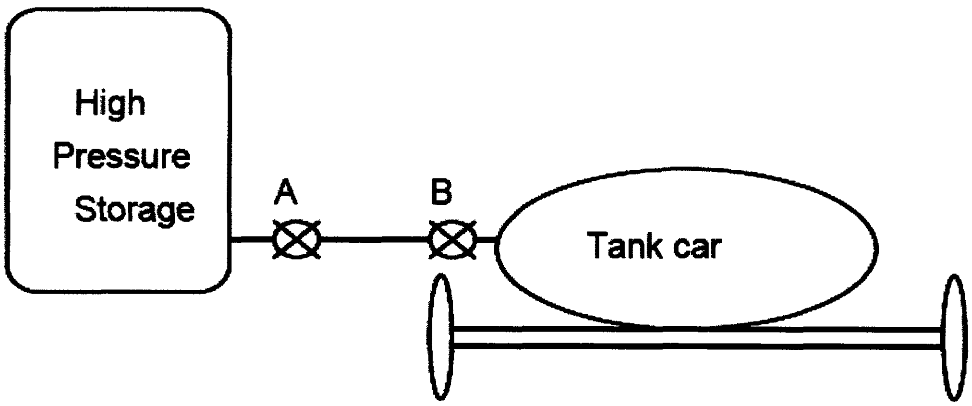

Figure 1: Schematic of normal configuration for filling tank car. Under optimal conditions, valve B is opened first so the air in the transfer line can be flush when valve A is opened and liquid begins to flow.

As the air column is compressed, the pressure in the segment of pipe spikes. The pressure oscillates as the air column acts as an air spring until the fluid comes to rest and the pressure reaches a steady state equal to the driving pressure of the storage tank. If the transfer line is simply designed to withstand this driving pressure, the swell in pressure could cause a rupture in the line and result in spilling hazardous liquid. It is therefore important to understand what factors influence the pressure surges so that the transfer line can be correctly designed based on maximum parameters.

To properly engineer a transfer line specific to the application, comprehension of the relevant parameters and the effects these have on the max line pressure is essential. In the previous incarnation of this experiment, the few parameters that were variable were driving pressure, hydrostatic pressure from varying heights of water in the tank, and the length of pipe between the valves (effectively transfer line length). The other major variable parameter was the opening time of the ball valve releasing the pressurized water into the transfer line. Because this valve was manually actuated, repeatability became a large factor in the system response.

In redesigning the experiment, the decision was made to include more variables and interesting phenomena in order to allow the students using the apparatus more freedom in developing their own experimental procedures. One major variable left out of the previous experiment was diameter. Many of the relevant equations are influenced by the ratio of diameter to length of the pipe. Also, by designing a sudden midstream change in diameter, the exploration (or at least the observation) of the effect of the reflected water at the boundary of the two diameters of pipe would be possible. Clear segments of pipe will aid the student in observing the oscillations occurring within the system and provide the possibility of adding a digital imaging facet to the experiment.

Apparatus and Procedure

The old experiment is pictured below. The filling tank was represented by a large tank on top of the lab bench that was filled with water and pressurized with air from a remote compressor. To simulate the transfer line, a section of pipe was segmented into two smaller sections by ball valves and separated from the tank by another ball valve. With this configuration (pictured in Figure 3), one could test two different lengths of pipe with a 180 degree bend added to the longer segment. The two lengths available were 1.7 m (67 in) and 3.1 m (122 in). A pressure transducer was plumbed into each segment at the terminus just before the ball valve.

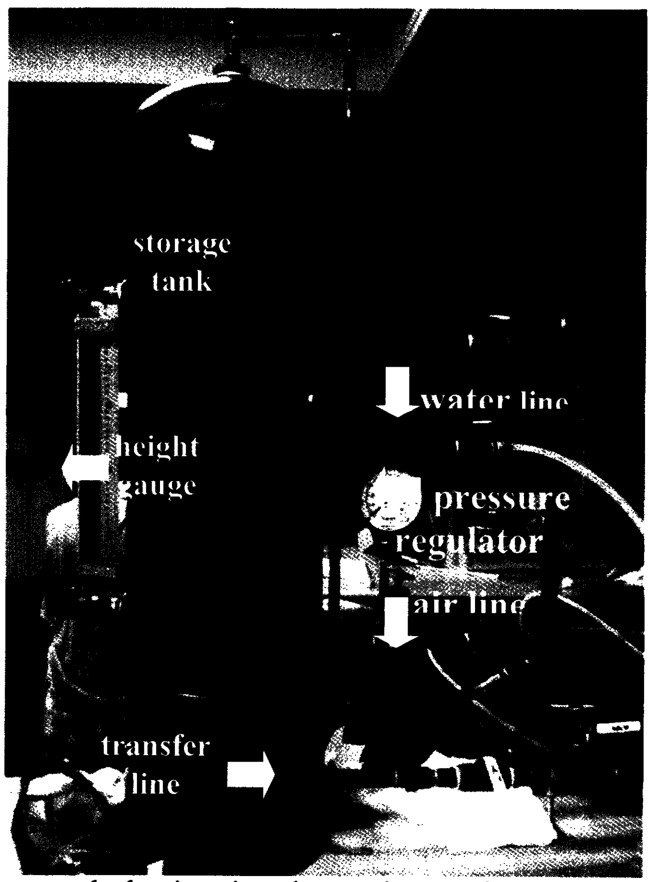

Figure 2: Storage tank showing air and water inputs. The air pressure is controlled and monitored using a pressure regulator. The height of the water is indicated by a gauge on the side of the tank.

There are many factors that went into the design of the updated experiment. Due to proprietary standards in the plumbing and pipe manufacture industries, the updated experiment is designed in English measurement units. For instance, pressure ratings for most common pipes and pipe fittings are provided in psi and pipe sizes are in inches (though the diameters are proprietary and are not necessarily the same as the industry accepted "size"). The old experiment has a very cramped and disorganized design that can confuse students as they try to develop a procedure for testing the apparatus. For this reason, an important design component for the new experiment is making the plumbing straight forward with a very clean layout.

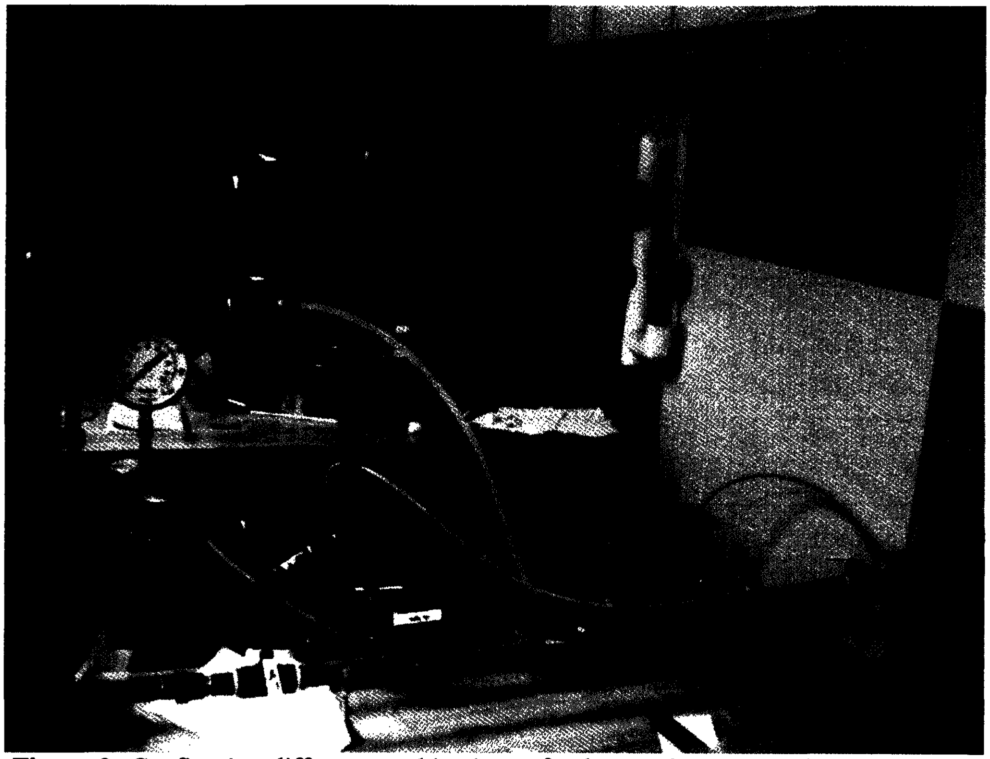

Figure 3: Configuring different combinations of valves and pipes simulate various transfer line configurations – a short transfer line and a longer one with a 180 degree bend. Pressure sensors near these valves are connected to a computer and monitor the pressure inside of the two transfer line configurations.

Because this is one of many of the 2.672 experiments that will be updated or replaced, the design also includes components that can be viewed as modular in that they can be easily used in other experiments. The other experiments can be more easily redesigned later using a similar holding tank if one is needed, and the optical workstation provides mobility, stability, and versatility for any future experiments. The idea of being able to use the very common parts in each experiment means students require less time to familiarize themselves with specific equipment and allows more time to be used in formulating the procedure. Also, because the new experiment as currently built serves as more of a bench level mock up, many of the components can be plumbed directly into the final version using the experiment built for this thesis as a blueprint.

The optical work bench will provide an ideal platform for the experiment, but to avoid drilling and tapping holes in the actual bench top, a piece of plywood is substituted and the mock up is built upon it. The base is on casters to allow the experiment to be easily swapped out with other future experiments so that the available experiments for 2.672 can change from semester to semester if necessary. Though the table is made for optical experimentation, this experiment does not require the vibration damping capabilities. The option, however, is available to add vibration isolators if other experiments later require the capability. The actual optical table top (not the plywood) has a matrix of ¼-20 tapped holes for easily securing experimental equipment. The model ordered does not have holes on the bottom, meaning that when the final version is constructed, holes will need to be drilled and tapped to allow the tank and other plumbing to be fastened beneath the table. A model can be ordered with custom hole configurations drilled and tapped on both top and bottom, but this was not a fiscally viable option, especially without having the final layout designed. A wide range of accessories are also available, if necessary, including mounts for computers, monitors, and other equipment. This versatility and mobility fit the modularity requirement of the redesign.

The tank on the old experiment has had to be replaced previously due to rust and corrosion. The new tank is epoxy lined to reduce corrosion, though similar models are available without epoxy lining for less money. This allows for the same tank to be used in other experiments where the tank must be filled with water while experiments without water can use a similar tank without epoxy to provide continuity from experiment to experiment. The tank is smaller than the previous experiment's tank. A ten gallon tank rated for 250 psi is adequate for any of the experiments currently in the lab.

The system in the mockup built for this thesis is plumbed in PVC piping for ease of construction without sacrificing pressure rating. In the diameters chosen for the experiment, schedule 40 PVC pipe has sufficient pressure rating for the available pressure ranges within the lab (maximum driving pressure of 80 psi with a new imposed limit of 50 psi for experiments).

	Max Operating Pressure (psi)	Min Burst Pressure (psi)
½"	358	1910
1"	270	1440

Table 1: Maximum operating and minimum burst pressures for schedule 40 PVC pipe according to ASTM D1785 "Standard Specification for Poly(Vinyl Chloride) (PVC) Plastic Pipe, Schedules 40, 80, and 120"

Though data acquisition hardware was not purchased for the mockup, information was compiled to facilitate choosing an appropriate model for later. Again, modularity was important in determining appropriate models. The envisioned format of the class includes students using their own laptops (or Institute provided laptops) in the lab. Therefore, USB connectivity is optimal. Also, models that interface with MATLAB's DAQ toolbox or are otherwise compatible with MATLAB are preferable due to the wide availability and common use throughout the Institute and department. Because students would be more able to manipulate MATLAB code than learn and manipulate LabView or proprietary software, students could again more easily create their own experiment. A table of appropriate models both for this experiment and for future experiments that may require more capabilities can be found in Appendix A.

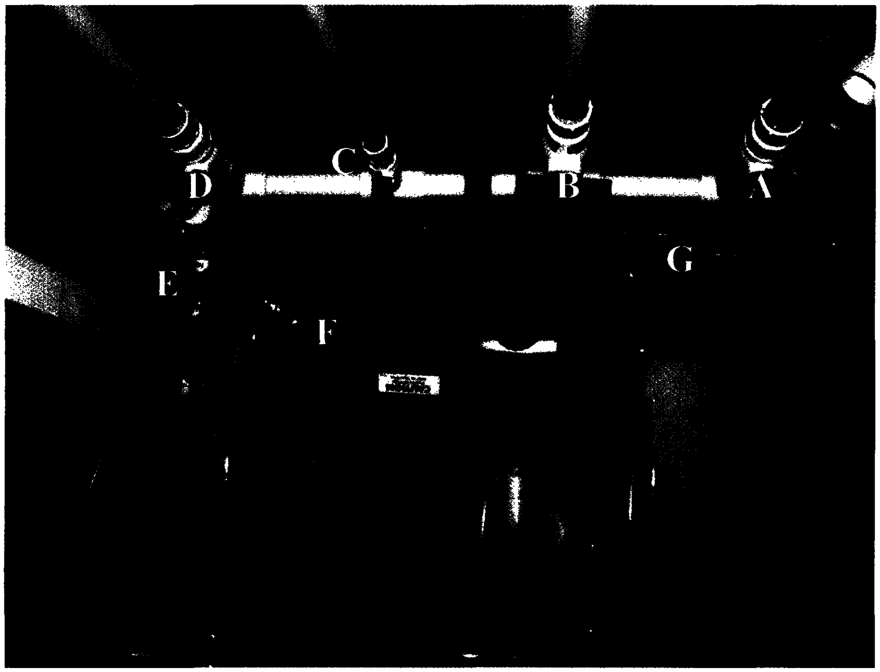

Figure 4: Tank placed below table. The red handles are part of the selection manifold for determining which "circuit" the water will enter before flowing to the top of the table. A) valve for selection circuit A; B) circuit B; C) circuit C; D) circuit D; E) drain valve for flushing circuits; F) water inlet from wall supply; G) air inlet manifold; H) drain valve for draining tank

In creating the general layout for the plumbing, placing the tank underneath the table cleared room above the table to neatly run the appropriate piping and allow for free work space. Also, in placing the tank under the bench, the water and air lines and associated plumbing could also be kept out of the way. While this dictates that several valves must also be located below the bench, the operation of those valves happens infrequently and should not prove terribly inconvenient. With more room above the table, configurations with more variables can be included in the experiment. Four different "circuits" are plumbed in the mockup; by opening or closing valves on two of these circuits, six different distinct arrangements can be tested.

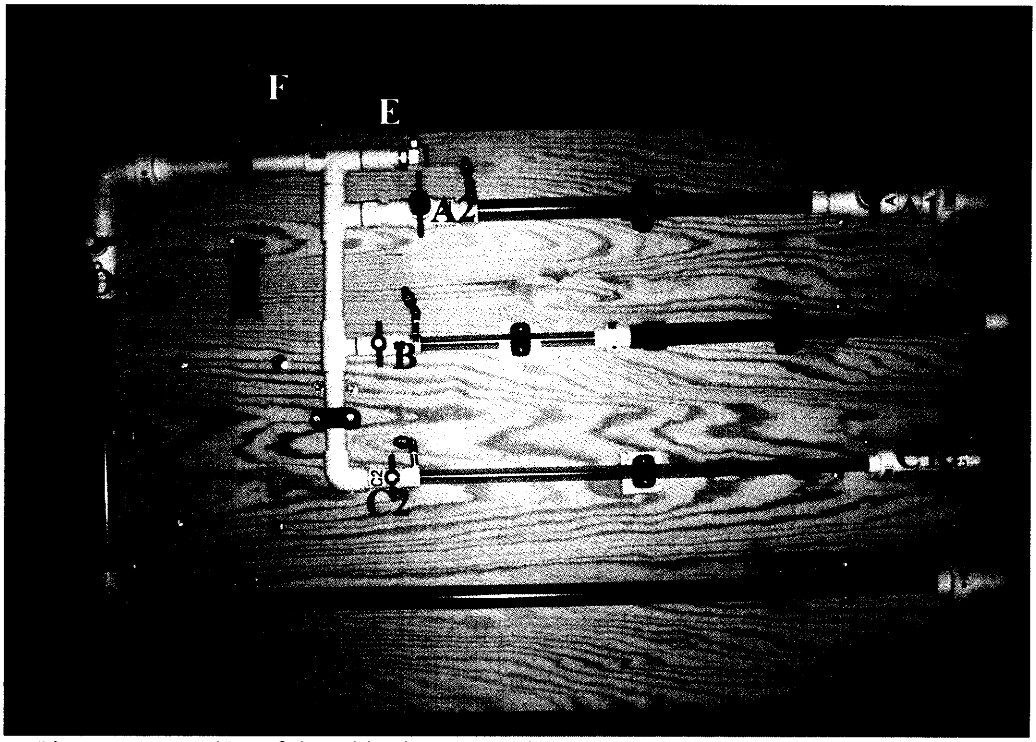

Figure 5: Top view of the table showing each circuit. Located near each ball valve are ports for connecting a pressure transducer. Clear sections of pipe all the oscillations of the water slug to be observed. A-D) correspond to A-D circuits from below the table; E) air diverted to flush the circuits to drain below table; F) pop safety valve rated for 275 psi.

All the "circuits" have a 180 degree bend where the piping is plumbed from below the bench to the top. The ports for the pressure transducer are all located above the table near the valve at the terminus of each configuration. The first circuit (A) is 1" pipe with two valves – one just past the 180 degree bend and one near the other end of the table. Circuit B is the same overall length as circuit A, but circuit B has an abrupt reduction to ½" pipe. Circuit C is similar to circuit A except that it is plumbed in ½" pipe to demonstrate the difference pipe diameter has on peak pressure – it like circuit A has two available lengths to test depending on whether its middle valve is open. The final circuit is a long section of 1" pipe that runs the entire length of the top of the table and has a 90 degree elbow that leads to its terminal valve.

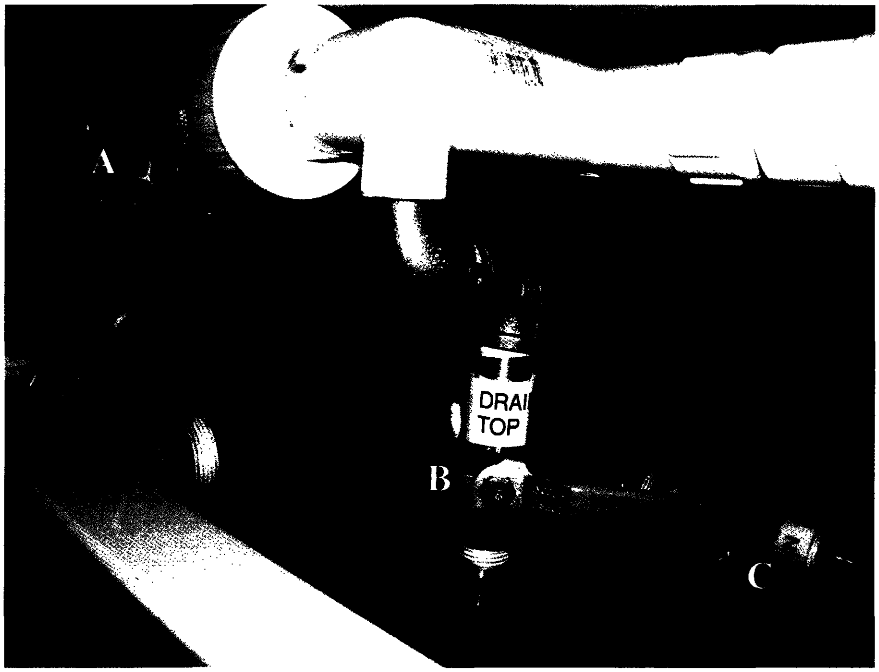

Figure 6: View of back side of plumbing underneath table. A) Solenoid valve for fast, repeatable release; B) valve for draining circuit manifold; C) water inlet to tank

The operation of the experiment is designed to be as straight forward and repeatable as possible. Before filling or pressurizing the tank, care should be taken that the manual relief valve, all drain valves, and the solenoid valve are closed. Once the tank is filled with water to the halfway point (visible through the sight window on the front side of the tank), the valve to the water line should be closed. A height gage is not included on this version of the experiment as the effect of hydrostatic pressure is minimal and predictable. Next, the tank should be pressurized using the air line, making sure that the 3-way ball valve is in the correct position to fill the tank instead of flush the system. A pop safety valve is connected and set to relieve the tank at 275 psi. To manually relieve air pressure, a valve is located near the pop safety valve.

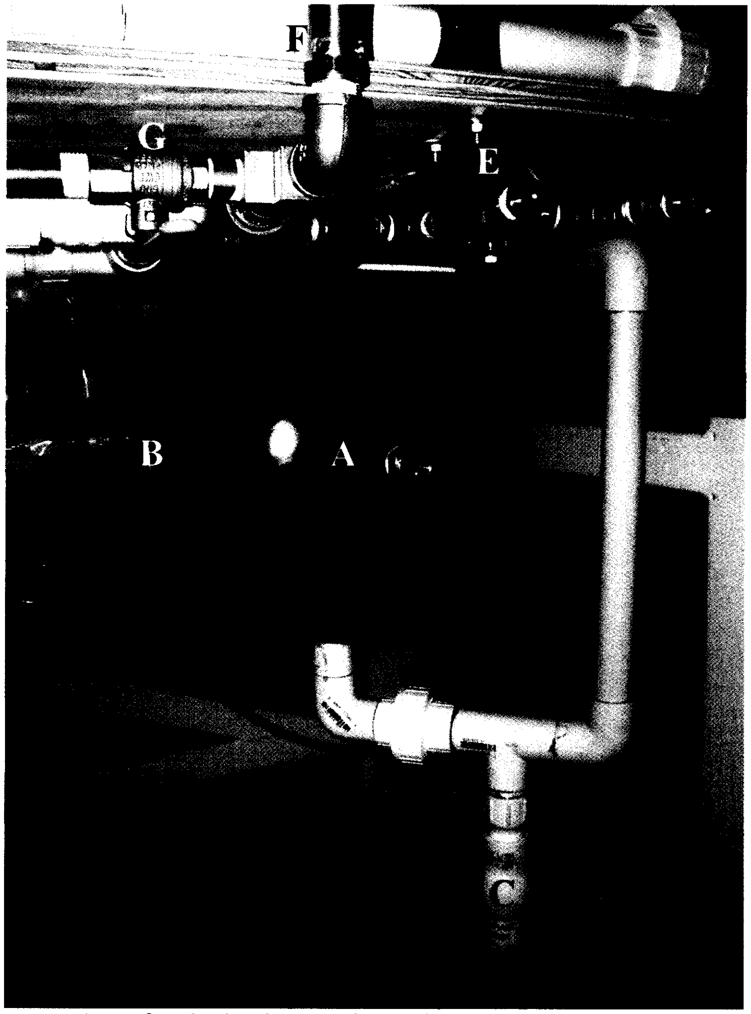

Figure 7: Front view of tank plumbing underneath the table. A) sight window for determining water level; B) water outlet to solenoid valve/circuit manifold; C) drainage valve for draining tank; D) air inlet to air manifold/tank; E) 3-way ball valve for diverting air to tank or to manifold above table to flush circuits; F) pop safety valve; G) exhaust valve for manually relieving pressure to tank

After the tank is filled and pressurized, the desired circuit can be selected for testing by turning the corresponding ball valve in the manifold to open while keeping the other circuits closed (the circuit is open when the handle to the valve is in line with the pipe and closed when the handle is perpendicular). The terminal valve above the table for the desired circuit should be closed and the pressure transducer plugged into the adjacent port. Other terminal ports should be closed unless they segment the desired circuit. Once the circuit is selected and the transducer is in place, the system will "fire" when the solenoid valve is actuated. The solenoid valve provides repeatability in place of manual valves. The solenoid valve should not remain open longer than necessary for the system to come to rest at its steady state driving pressure.

To drain only the tested circuit, open the drain valve located near the manifold below the table. Then by turning the valve at the air line inlet, air is forced into the manifold above the table at the terminal of each circuit. One only needs to turn the terminal valve for the circuit he wishes to flush to allow the air to push the water back down to the drain. Once draining of the circuit is complete, close the terminal valve, switch the air pressure back to the tank, and close the drain valve. The system is once again ready to "fire."

Once all experiments are complete, the tank is drained by opening the drain valve at the bottom of the tank while the air pressure is still switched to the tank. After all the water is drained, shut off the air pressure valve from its source at the wall and relieve pressure to the tank by opening the manual relief valve.

Theoretical Analysis

Developing a theoretical model that associates the significant parameters to transfer line pressure reveals the effect each parameter has on the peak pressure. The model developed below is based on the old experimental setup, but is still relevant because the major difference is in hydrostatic pressure loss from different pipe height. This is easily corrected by adjusting *h* to take the height change of the pipes into account. The peak pressure occurs as the flowing water compresses the air trapped between the water and the closed valve (B in Figure 4, not related to labeled circuitry in above figures). The column of air acts as a spring and forces the water back towards the tank. This all happens very quickly (the first rebound happens within approximately half a second), so valve A is not completely open before the water rushes past and is subsequently rebounded. The resistance of the partially closed valve skews the damping characteristics of the system as the pressure drop across the valve reduces as it opens.

The unsteady Bernoulli equation provides a correlation between the pressure (*P*) at different points in the defined system and physical parameters such as gravity, height, and flow velocity (*v*) (Equation 1).

$$\int_1^2 \frac{\partial v}{\partial t} ds + \int_1^2 \frac{dP}{\rho} + \frac{1}{2}\left(v_2^{\,2} - v_1^{\,2}\right) + g\left(z_2 - z_1\right) = 0 \qquad (1)$$

Because Equation 1 depends so heavily on the streamline (*ds*) and the points 1 and 2 that the pressures are integrated between, it is essential to first define these points before the equation can be used.

To simplify the integration along the streamline, a streamline that exhibits near linear flow is estimated to start very close to the bottom of the tank (Figure 4). This choice of streamline eliminates the need to solve the first integral in Equation 1.

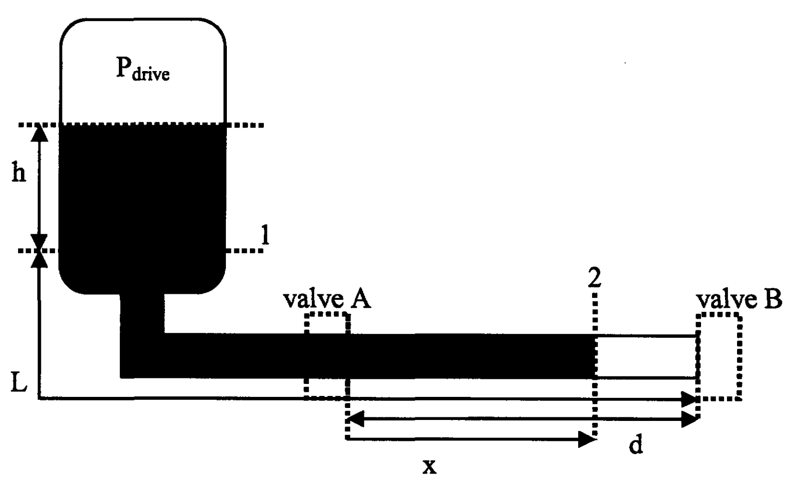

Figure 8: Illustration showing coordinate selections and distance naming conventions. The choice of state 1 is important for the integration of the first integral in Equation 1 due to flow along the streamline from this point.

This simplified streamline choice makes the integration in terms of *ds* possible analytically – merely the length of the streamline according to the above definitions, L (Equation 2). The continuity equation (Equation 3) shows that v_1 is virtually equal to zero due to the large difference in diameter between the tank and the pipe and the incompressibility of water ($\rho_1 = \rho_2$).

$$L\frac{dv}{dt}+\frac{v_2^{\ 2}}{2}+\frac{P_2-P_1}{\rho}+g(z_2-z_1)=0 \tag{2}$$

$$(\rho Av)_1=(\rho Av)_2 \tag{3}$$

P_1 is easily found by adding the regulated driving pressure of the air, P_{drive}, and the hydrostatic pressure of the water above the beginning of the streamline, ρgh. The change in height along the streamline is negligible and can be ignored. P_2 and v_2 remain the only unknown variables in this equation. However, because this oscillation takes place too rapidly for heat transfer to occur with the surrounding environment, the process can be modeled adiabatically. The pressure of the air is the same as the pressure of the water at the interface, so modeling the air adiabatically provides P_2 (Equation 4).

$$P_{atm}V_{atm}^{\ \gamma}=P_2V_2^{\ \gamma} \tag{4}$$

Here, γ is the adiabatic constant, which is equal to 1.4 for air. P_{atm} and the associated volume refer to the air between valve A and valve B before valve A is opened; the air column is at atmospheric pressure. Because the cross section of the pipe is constant, equation 4 can be reduced to a function relating P_2 to position of the water-air interface (Equation 5).

$$P_2=P_1\left(\frac{V_1}{V_2}\right)^{\gamma}=P_1\left(\frac{d}{d-x}\right)^{\gamma} \tag{5}$$

Now it is important to recall the damping the ball valve and elbows cause on the oscillations. This damping is the result of a phenomenon referred to as head loss. Head loss is the pressure drop caused by the impedance of flow due to friction or general obstruction. Major head loss is created by viscous forces along the pipe walls. Minor head loss results from obstructions, bends, and pumps. However, the name major head loss is a bit deceiving as the minor losses dominate this particular situation. The Darcy-Weisbach equation (Equation 6) shows that the major head loss is very dependent on the ratio of length to diameter of pipe (L/D) and is proportional to the velocity squared. Because the coefficient for laminar flow is very small and the experiment will take place largely in the laminar region, it is helpful to neglect the major head losses. The pressure drop due to minor head loss, $\Delta P_{h,\min or}$, is proportional to the pressure due to the velocity of the fluid by a constant, K, which is specific to the kind of obstruction causing the pressure drop (Equation 7).

$$\Delta P_{h,major}=\lambda\cdot\frac{L}{D}\cdot\frac{\rho v^2}{2} \tag{6}$$

$$\Delta P_{h,\min or}=\frac{1}{2}K\rho v^2 \tag{7}$$

By dividing Equation 7 by the density, ρ, subtracting it from Equation 2, substituting for P_2, and simplifying, one is left with an ordinary differential equation that is easily solved using MatLab (Equation 8). Because x is measured from valve A and the air-water interface begins at valve A, both x and v are initially zero.

$$\frac{dv}{dt} = \frac{1}{L}\left(\frac{(P_1 - P_2)}{\rho} - \frac{(K+1)}{2}v^2\right) \tag{8}$$

Once MatLab returns values for the position, x, with relation to time, this can be plugged back into Equation 5 to produce values of pressure in the transfer line with respect to time. The maximum pressure can then be determined graphically or by using MATLAB's max() function.

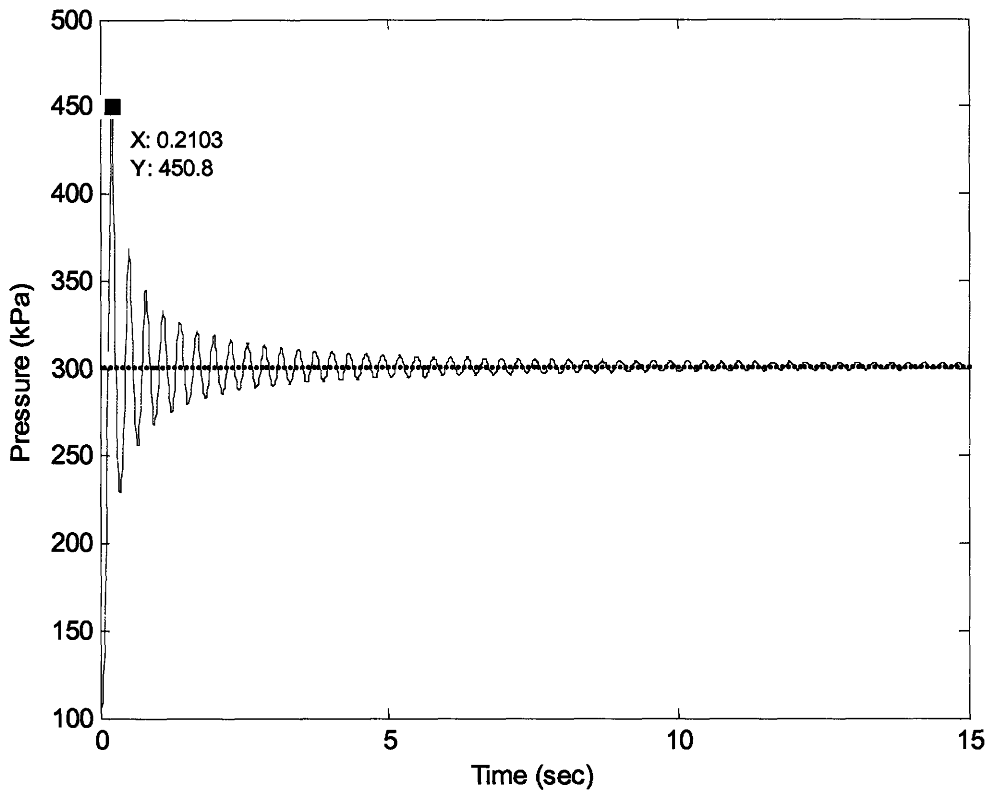

Figure 9: This graph shows the theoretical pressure as valve A is opened and the resulting peak pressure. This data is for the following parameters: K = 8, L = 1.7 m, d = 1.18 m, h = .1 m, P_{drive} = 200 kPa. The dotted black line shows the steady state pressure derived from the driving pressure (200 kPa) plus the hydrostatic pressure (ρgh). *Note: P_{drive} is gauge pressure while the sensor records absolute pressure.*

	Driving Pressure		
	200	**300**	**400**
short	452.8	659.2	890.1
long	406.4	575.6	759.9

Table 2: Theoretical values of peak pressure for the 18 different configurations tested on the old experiment, averaged according to drive pressure and pipe length due to negligible hydrostatic pressure. All pressures are in kPa. Trends show that driving pressure has the most significant effect on peak pressure.

Peak pressures for the redesigned experiment can be determined by using the model and script that were developed for the older experiment and simply substituting values of length and impedance for the new layout. Because the chief concern is whether the new design will produce peak pressures greater than the burst pressure of the PVC pipe used, there is no need to calculate peak pressures at each possible pressure that a student may test. Instead, driving pressures of 50 psi and 80 psi were used to calculate the corresponding peak pressures as these are the maximum pressure allowed in lab and the maximum output pressure from the wall, respectively. Though students should not be allowed to drive the system at 80 psi, for safety reasons the experiment should be robust enough to withstand that pressure.

	Driving Pressure			
	50 psi		80 psi	
	psi	kPa	psi	kPa
A1	103	611	154	1059
A2	98.6	580	145	99.7
B	99.1	583	145	1003
C1	108	645	164	1130
C2	99.8	588	147	1010
D	81.8	564	141	962

Table 3: Theoretical values of peak pressure for each "circuit" of the redesigned experiment (circuits are labeled A-D with bisected circuits labeled with a corresponding 1 and 2). The peak pressures are presented in psi for comparison to the burst pressure of PVC provided in Table 1 and also in kPa for comparison to peak pressures produced in the older model of the experiment.

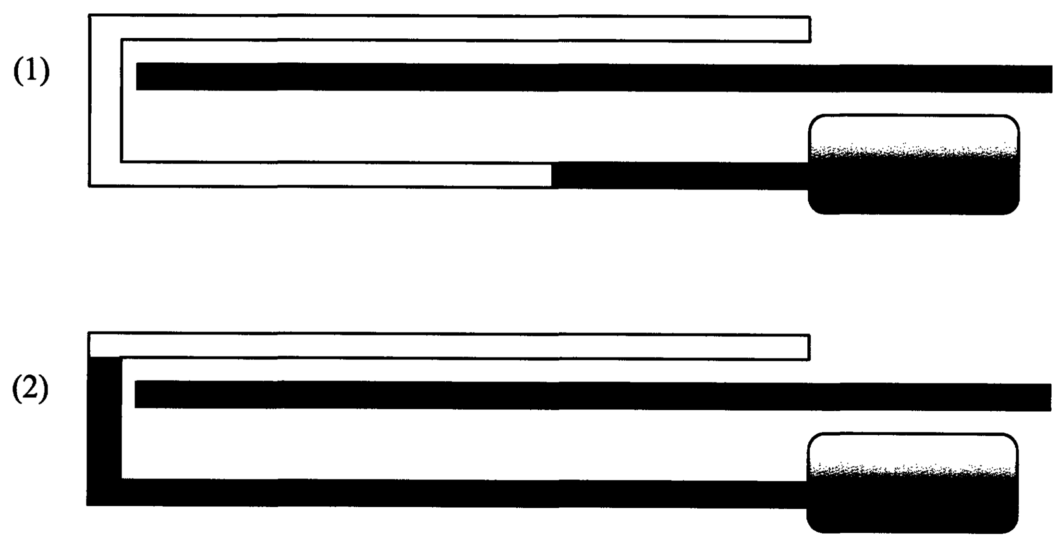

Figure 10: Simplified states 1 and 2 used to determine resting level of the water after the experiment has completed. Because the bends in the piping do not effect the final column of air, they could be left out of the simplified version as long as the relevant volumes were still considered.

Upon testing the experimental setup, it became evident that the intended operating pressure ranges were not sufficient to produce the visual effects the clear piping was supposed to demonstrate. The level that the water came to rest was below the level of the top of the table. In looking at equations to determine the factors that caused this to happen, the end condition was considered independent of the operating time. In assuming that the transition from initial to final conditions happens over sufficiently long enough time for heat transfer, the adiabatic condition used in earlier equations is not used and instead a more simple equation is utilized (Equation 9).

$$P_1V_1 = P_2V_2 \tag{9}$$

The pressure and volume of the column of air at the end of the pipe that is being compressed in the experiment is considered here. The resting level of the water can be determined by finding the volume of air in state 2. Because the maximum difference between the driving pressure and the pressure of the air in the end of the pipe in state 2 is negligible (roughly .3 psi), the pressure of the air column in state 2 can be taken as the driving pressure in the tank – keeping in mind that the driving pressure is gauge pressure. The cross section of the pipe remains constant, so by substituting into Equation 9 and simplifying, the length of the column of air can be found as a function of driving pressure.

$$L_2 = \frac{P_{atm}}{P_{drive} + P_{atm}} \cdot L_1 \tag{10}$$

Using 50 psi as a maximum operating pressure, the length of the air column comes out to be 18 inches. The length of the pipe above the table used in the equation was 23 inches, so roughly 20% of the clear pipe above the table will be filled with water when the experiment comes to rest after running it at maximum pressure. This is an insufficient amount of water to produce the oscillating water slug visual effect that the clear pipe is supposed to demonstrate.

Experimental Results

Due to lack of DAQ hardware, data were not collected for the mockup of the new layout. The following is from experimentation done on the old setup to validate the theoretical model, which then allows the model to be applied to the mockup. At the time the original experiment was run, the limit of 50 psi had not been instituted, so it was driven at a maximum of 500 kPa (or 72.5 psi).

The experimental data followed the physical intuition of the model very closely. As seen in the graphs below, the pressure peaks as soon as the valve is opened; the transient is damped out within an average of 5 seconds and comes to rest near the steady state pressure (drive pressure plus hydrostatic pressure).

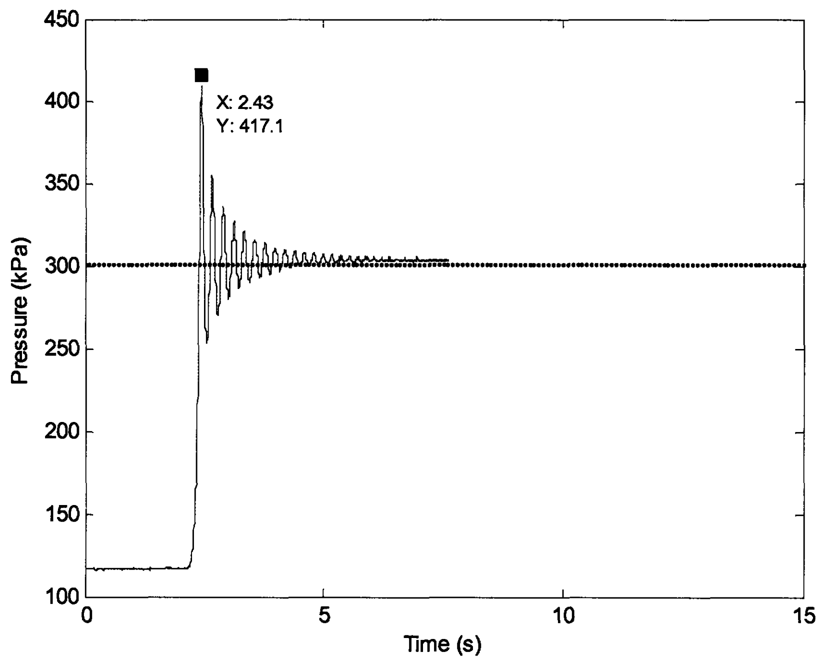

Figure 11: This graph shows the theoretical pressure as valve A is opened and the resulting peak pressure. This data is for the following parameters: K = 8, L = 1.7 m, d = 1.18 m, h = .1 m, P_{drive} = 200 kPa. The dotted black line shows the steady state pressure derived from the driving pressure (200 kPa) plus the hydrostatic pressure (ρgh). *Note: P_{drive} is gauge pressure while the sensor records absolute pressure.*

The peak pressure scales as the driving pressure. The water height adds a negligible amount of hydrostatic pressure – 1-3 kPa hydrostatic as opposed to the 300-500 kPa driving pressure. Due to the small contribution of the water height, Figure 7 shows the peak pressure each length of pipe produced for a given driving pressure averaging results for different water heights.

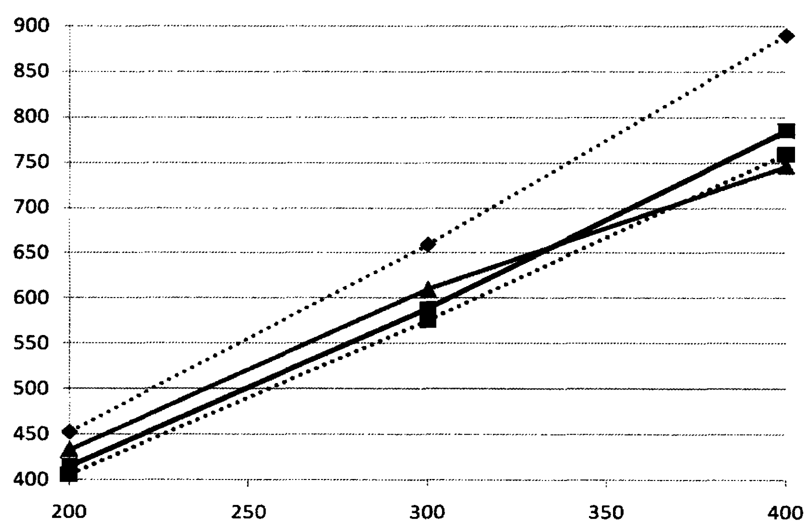

Figure 12: Averaging across all water heights, peak pressure as it relates to driving pressure for each length of pipe. The theoretical results are dashed while the experimental results are in solid lines. The short length of pipe is represented by the blue lines while the longer pipe is in red.

While the long section of pipe is very closely modeled by the theory, the short section does not behave as expected at higher pressures. The trend fit to the experimental data shows the peak pressure increasing at a decreasing proportion to the driving pressure for the short pipe. This is counter intuitive and has a few possible reasons given the experimental setup. Looking at the results for 400 kPa on the short section while treating each different hydrostatic pressure as merely another experimental trial keeping the other two variables constant, it is clear that major discrepancies between trials occurred (likely speed of valve turning). The same is true for each length of pipe compared to driving pressure, taking each height of water as identical trials. When the standard deviation between different experimental peak pressures for each water height for the same conditions (for instance 400 kPa, short section) is divided by the average peak pressure for those conditions, the long section of pipe has between 2% and 6% deviation from the norm while the short pipe is between 6% and 10%. When the same thing is done for theoretical peak pressures, the difference in water height produces less than 1% standard deviation in every circumstance. Therefore, the discrepancies cannot be attributed to merely averaging the water height data. In the discussion section, possible reasons for the discrepancies will be discussed as well as why the longer section experienced less variance.

Discussion

The theoretical model very accurately describes the experimental results with an average error of -3.3%. The model for the short valve distance often predicted a higher peak pressure with an average of -9.3% error while the model for the longer valve distance predicted closer peak pressures with an average of 2.65% error.

		200			300			400		
		0.1	0.2	0.3	0.1	0.2	0.3	0.1	0.2	0.3
theory	short	450.8	452.8	454.8	657.0	659.2	661.3	887.7	890.1	892.4
	long	405.0	406.3	407.9	573.9	575.6	577.3	758.1	759.9	761.8
exper	short	427.0	415.8	457.5	554.0	677.3	600.4	691.9	779.8	766.4
	long	422.5	404.5	420.2	571.9	566.2	628.0	736.9	832.4	787.5
% error	short	-5.3	-8.2	0.6	-15.7	2.7	-9.2	-22.1	-12.4	-14.1
	long	4.3	-0.4	3.0	-0.3	-1.6	8.8	-2.8	9.5	3.4

Table 4: Theoretical and experimental peak pressures for each experimental variation. The percent error was calculated by subtracting the theoretical from the experimental and dividing by theoretical.

Though the discrepancy between the two experimental setups is slight, it points towards slight inaccuracies in the model. For instance, the value of K for the partially opened ball valve was arbitrarily determined and could not be great enough to provide enough damping in the model. The impedance of a partially opened ball valve varies greatly depending on the percent the valve is opened. During the experiment, control over the rate at which the ball valve was opened could have had a significant impact on the value of K. According to the current theoretical model, the K value for the 180 bend is added directly to the K for the ball valve. Therefore, by this method, the long setup would be skewed while adjusting the K value for the shorter setup. However, closer inspection and a more elaborately conceived model would reveal that with a longer transfer line, the rebounding water is not as greatly impeded by the ball valve due to the greater distance between valves. Because the water in the mockup travels so far from the valve before rebounding, the theoretical values for peak pressure should not be effected in the same way the longer lengths of pipe in the original experiment were not effected.

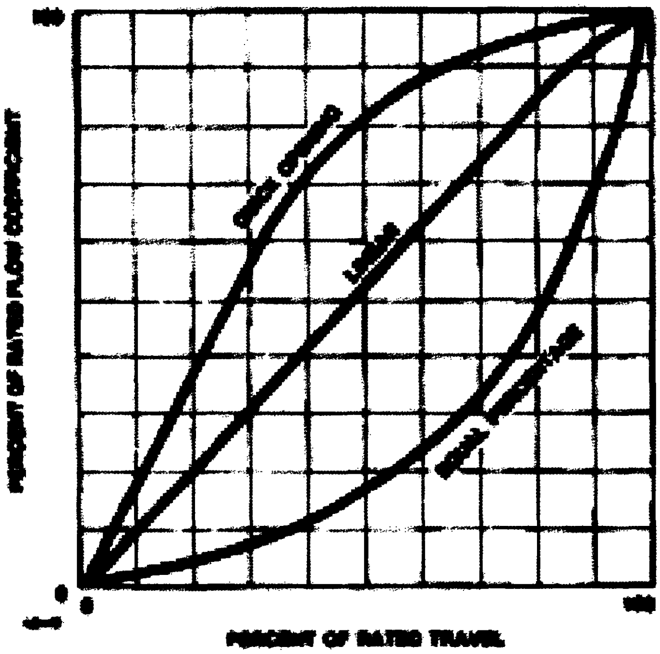

Figure 13: Graph illustrating relationship between percentage ball valve is open and flow coefficient (related to K) for a standard ball valve. There is a characteristic difference between different methods of opening the valve. (Taken from flowbiz.com)

Even when the more accurate long transfer line setup is compared to the theoretical, there is a physical discrepancy in the dynamic response. Figure 10 shows that the response begins very similarly – the pressure peaks immediately after the valve is opened, but the experimental takes much less time to damp down to a steady state value. Assuming more accurate determinations of the K value for the transfer line were made, there are still other considerations to take into account before this experimental model can accurately predict the secondary response. When dismissing major head loss in previous equations, the small significance of this pressure loss was attributed to the laminar flow during the experiment for all maximum driving pressures. The major head loss becomes significant when the peak pressure drives the water at a higher pressure than the maximum driving pressure and creates turbulent flow. Because the flow becomes turbulent after the pressure spike, major head loss quickly creates a pressure drop that damps out the secondary response as well. The major head loss is determined by the velocity, though, so the solution becomes iterative. Because the most relevant information safety-wise is the peak pressure in the line, the inaccuracies modeling the damping over time and the effect of major head loss is still somewhat irrelevant.

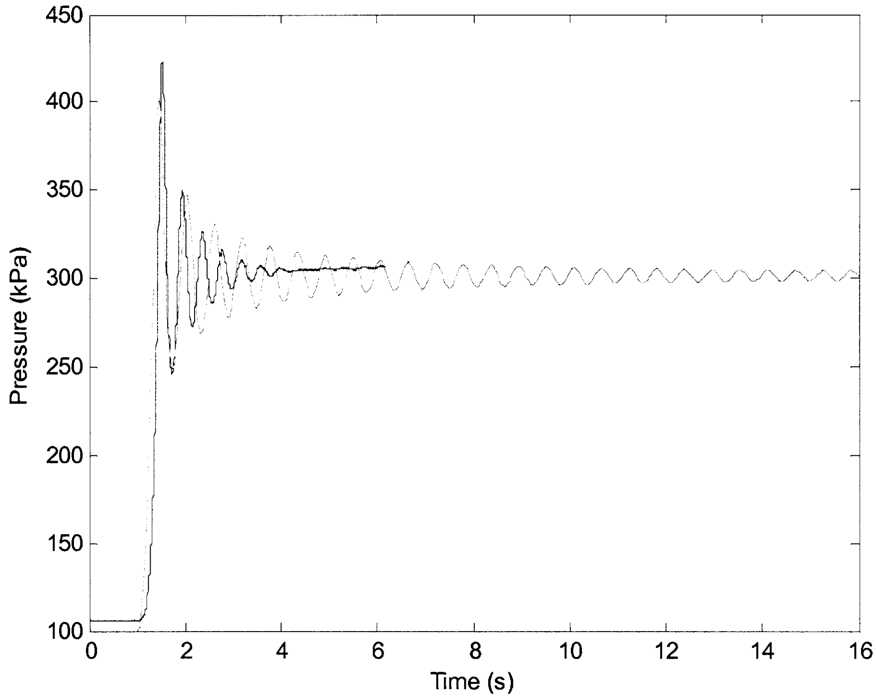

Figure 14: Pressure vs. Time graph of theoretical and experimental data. The theoretical response takes much longer to damp out. Data is for K = 10, L = 3.1 m, d = 2.5 m, h = .1 m, and P_{drive}= 200 kPa (gauge).

To use this model to evaluate actual transfer line robustness, actual conditions for transfer lines should be explored. Tanks can be on the order of 30 meters tall which when full of water results in a hydrostatic pressure on the order of 300 kPa. This pressure is equal to the minimum driving pressure tested and is very likely sufficient to drive the transfer of fluid from tank to car. A common material used as transfer lines is ultra high molecular weight polyethylene (UHMWPE), which has a working pressure of 1.4 MPa. This tubing comes in standard lengths of 30 meters; at this length, the prior assumption that major head loss could be discounted is not as valid. By first calculating the velocity without major head loss and then using this velocity in the Darcy-Weisbach equation, the MATLAB script can be run again including an estimate for major head loss and closer peak pressure can be estimated. For a liquid with a density similar to that of water and assuming the same K value for valves (though minor head loss now becomes the insignificant term), this peak pressure is roughly 1.5 MPa. A safety factor is usually designed into piping and tubing to resist bursts from peak pressures, so this over pressure of less than 10% should not rupture the line.

The mockup sufficiently demonstrates the necessary plumbing for operation and spatial configuration of all components. Some things will need to be modified for the final version of the lab, both for functional and aesthetic purposes. For instance, the height of the table was insufficient for both comfortable use and spatial configuration of all necessary equipment. For this reason, the mockup has spacers lifting the table 6 inches. When the table is raised onto its feet and off its casters, it will gain another 4 inches. This extra room and more permanent risers should provide ample room to access and operate valves below the table as well as provide clearance for the equipment above the floor. Also, the manifold beneath the table should be plumbed with the valves rearranged as in Figure 14. The way the valves are currently arranged, the water slug travels all the way down towards valve A, then rebounds and travels through the selected circuit. By rearranging the valves, the flow would only travel to the valve that is open and follow that piping to the top.

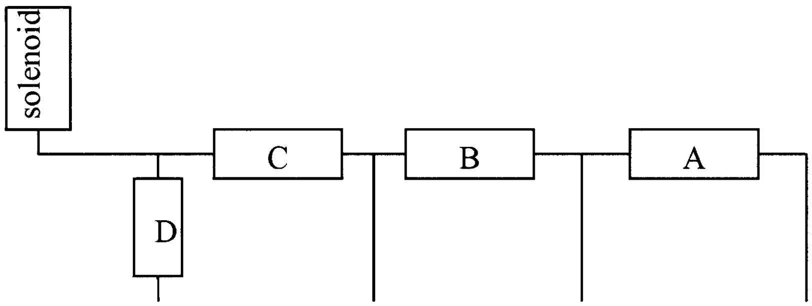

Figure 15: Improved valve placement for bottom manifold.

The equation to determine the length of the final air column can be used as a maximizing equation in redesigning the length of pipes for the next version of the experiment. One way to improve this arrangement is by shortening the length of pipe underneath the table by moving the manifold in Figure 14 to the edge of the table. This would serve two functions: the valves would be easier to operate as they could be positioned right near an edge instead of in the middle of the table underneath, and the column of air being compressed would be shorter and would begin near the top of the table anyway, so the oscillations would definitely occur visibly in the clear sections of pipe. The plumbing underneath would just involve either positioning the tank nearer the middle of the table (underneath) with the manifold plumbed a short way from it right near the edge. Alternately, the tank position can stay similar to its current placement for ease of connecting it to the wall (for air and water) and a single pipe can be run between the manifold and the tank. So instead of having four long pipes spanning the bottom of the table, only one would span the entire length of the table underneath. The length of the pipe between the tank and solenoid valve/manifold is practically irrelevant, though the air in this pipe becomes significant as the line is first charged. Inclusion of a bleed valve just before the solenoid valve so the air compressed between the water and solenoid valve can escape would render this length of pipe completely irrelevant for the experiment's purposes.

For aesthetic purposes, PVC could be replaced with copper tubing or any number of piping materials. White PVC has a tendency to develop a dirty look, though the PVC is functionally adequate to perform all necessary operations of the experiment. The solenoid valve used is intended for a home sprinkler system, but could be replaced by a solenoid intended for a dump tank. A solenoid valve similar to the Series 80 from Peter Paul Electronics Co., Inc., would be ideal as it is intended for high flow, requires little (5 psi) differential pressure to open, and can resist up to 150 psi maximum differential pressure.

Also, a DAQ should be purchased and installed to the table with the pressure transducer properly wired to it. The solenoid valve should also be wired, possibly with a switch; depending on the capabilities of the DAQ, the solenoid valve may be able to be triggered by the DAQ which would help in timing the recording of the pressure from the transducer. Additionally, various plumbing differences will be necessary when installing the actual optical table work surface, as it is thicker than the current plywood mounting surface. Pipe supports that hold the plumbing further off the mounting surface (the air manifold in particular) should also be investigated to facilitate easier access to loosen or tighten union joints as necessary.

Conclusions

The theoretical model developed herein works well for quickly estimating how various factors qualitatively affect the peak pressure in a storage tank transfer line, even though scaling these factors up to realistic proportions renders some assumptions invalid. However, starting from the software developed to determine peak pressure in this experiment, modifications can easily be made to more accurately model the realistically proportioned situations and predict a more accurate peak pressure. Optimization software can be created to accurately determine most favorable, safest parameters for transfer line operation. For instance, by inputting the tank height, estimated valve interference, maximum operating pressure for the specific material hose being used, and the density and viscosity of the fluid being transferred, the maximum length for the transfer line can be readily returned within a specified safety factor.

The experiment itself, though not in its current state, proved useful in investigating different factors that affect the peak pressure. Producing a mockup from cheaper, easier materials to work with was a more efficient way of developing the basis for the final model. Rather than using copper tubing and the original table top for the optical table, PVC and plywood allowed more freedom to make changes as complications arose. Though there are still some problems with spatial arrangement underneath the table, these can be worked out easily when constructing the final version using this mockup as a blueprint. Various relevant factors that only became relevant after testing this mock up can be changed for the next version using optimization equations and by considering how change in these factors may create similar situations elsewhere in the plumbing.

Acknowledgements

This report, as it related to the "old" 2.672 experiment, was prepared based on experiments conducted with Adam Kaczmarek and Sean Schoenmakers. The advice and guidance of Prof. Todd Thorsen was instrumental in deriving relevant theoretical models. Prof. Doug Hart led the redesign and the input from Dr. Barbara Hughey and Brian Ruddy helped form the groundwork for the layout of the mockup. Dick Fenner was an invaluable resource in both plumbing expertise and general guidance.

References

Accord International, Inc. Rubber Hose. (Product Information site for transfer lines) http://www.accordintl.com/rubber%20hose.html

Cravalho, Ernest G. et al. Thermal Fluids Engineering. Oxford University Press, 2002. (Fluid Dynamic equations)

FlowBiz VA. Rotary Valve Design for Control Applications. (Ball valve K-value relationship) http://www.flowbiz.com/VA/designs.htm

PIPE-FLO Professional. Method of Solution. (Pipe flow equations). http://www.eng-software.com/products/methodology/pipe_flo.pdf

APPENDIX A – Data Acquisition (DAQ) Hardware Selection Table

Company Name	Model	Channels (analog)	Bits A-to-D	Sample rate (kS/s)	Price	notes
Data Translation	DT9812-10V	8 SE	12	50	$299.	non-isolated ground
Data Translation	DT9813-10V	16 SE	12	50	$349.	non-isolated ground
IO Tech	Personal DAQ/56	20 SE / 10 DI	up to 22	< 80 Hz @22 bit, 1 MHz less res	$1199.	may not be matlab supported, but is stackable
IO Tech	Personal DAQ/3005	16 SE/ 8 DI	16	1000	$1399.	expandable up to 64 SE/ 32 diff
Measurement Computing	miniLAB 1008	8 SE/ 4 DI	12	1.2	$109.	$99 for orders of 5-9, price drop above 10
Measurement Computing	USB-1208FS	8 SE/ 4 DI	12	50	$149.	
Measurement Computing	USB-1408FS	8 SE/ 4 DI	14	48	$249.	
Measurement Computing	USB-1608FS	8 SE	16	200	$399.	discount for orders > 5
Measurement Computing	USB-1616FS	16 SE/ 8 DI	16	200	$799.	daisy chain-able
NI	USB-6008	8 SE / 4 DI	12	10	$159.	
NI	USB-6009	8 SE / 4 DI	14	48	$269.	
NI	USB-6210	16 SE / 8 DI	16	250	$499.	
NI	USB-9201	8 SE	12	500	$529.	
NI	USB-9221	8 SE	12	800	$669.	
NI	USB-6218	32 SE / 16 DI	16	250	$1099.	
NI	DAQPAD 6015 (USB)	16 SE / 8 DI	16	200	$1299.	
NI	USB-6251	16 SE / 8 DI	16	1250	$1349.	
NI	USB-6259	32 SE / 16 DI	16	1250	$1899.	

APPENDIX B – MATLAB script that returns theoretical data based on different parameters

B1. Code setting up a system of differential equations. Parameters were changed manually within the code to model each experimental setup.

```
function dydt = ydot(t,y)
x = y(1);
v = y(2);

%head loss coeff
K = 8;
%K = 10;

%pipe length
L = 1.7;
%L = 1.7+1.355;

%space between valves
d = 1.1811;
%d = 1.1811+1.355;


%height of water
h = .1;
%h = .2;
%h = .3;

%driving pressure
P1 = 300e3;
%P1 = 400e3;
%P1 = 500e3;


g = 9.8;    %gravity
rho = 1000; %density of water
P = 1e5;    %atmospheric pressure
gamma = 1.004/.717;    %adiabatic gas constant

P2 = P*(d/(d-x))^gamma;

dydt(1,1) = v;
dydt(2,1) = (1/L)*((P1+rho*g*h-P2)/rho - v*(v)/2 - K*v*abs(v)/2);
```

B2. Code that integrates ODE's in Appendix B1, then takes the position vector returned and converts to pressure of the air in the transfer line (P2). Each pressure and time vector returned were then written to a text file using a number scheme to denote the different parameter configurations.

```
clear all

thisone = [input('filename: ','s') '.txt'];

d = 1.1811;
d = 1.1811+1.355;

[t,y] = ode23('ydot',[0 15],[0 0]);
P = 1e5;
gamma = 1.004/.717;
for n=1:size(t)
   P2(n) = P*(d/(d-y(n,1)))^gamma;
end
dlmwrite(thisone,P2,'delimiter',' ');
dlmwrite(thisone,t,'-append','roffset',1,'delimiter',' ');
```

B3. Code that reads text files containing pressure data for each experimental setup, determines the maximum, and returns a matrix of all peak pressures for all setups.

```
clear all;

% i: 1=short, 2=long
% j: 1=10 cm water, 2=20 cm, 3=30 cm
% k: 1=200 kPa (gauge), 2=300 kPa, 3=400 kPa


for i=1:2
   index=1;
   for j=1:3
      for k=1:3
         m=dlmread(['p' int2str(i) int2str(j) int2str(k) '.txt'],' ');
         temp = m(1,:);
         P2(i,index) = max(temp);
         index = index+1;
      end
   end
end
```